

Original Article

Time-dependent toxic effects of N-ethyl-N-nitrosourea on the testes of male C57BL/6J mice: a histological and ultrastructural study

Jun Yin^{1,2}, Kaiwen Sun², Bing Chen^{1,2}

¹Comparative Medicine Center, Yangzhou University, Yangzhou 225009, Jiangsu, PR China; ²College of Veterinary Medicine, Yangzhou University, Yangzhou 225009, Jiangsu, PR China

Received December 14, 2014; Accepted February 5, 2015; Epub February 1, 2015; Published February 15, 2015

Abstract: N-ethyl-N-nitrosourea (ENU), a well known alkylating agent, is a powerful mutagen in mouse spermatogonia that is frequently used to generate mutant mice for the study of gene function. The present study was performed to investigate the toxic effects of a suggested ENU treatment protocol (100 mg/kg ENU once a week for three consecutive weeks) on the C57BL/6J mouse testis using light and transmission electron microscopy, with reference to testis weight and sperm count. Time-dependent changes in the weight of the testes, sperm counts and testicular morphology were observed, following an injury and recovery pattern; the most severe damage was observed in week four after the first injection of ENU, and then the testis gradually recovered. By the end of the experiment (week 12), the testis weights and sperm counts of the ENU-treated mice had restored to around 80% of the respective values in the control group. Histopathological alterations in the testis were identified by light and electron microscopy, which revealed that ENU led to a temporary depletion in the number of spermatogenic cells via direct and indirect toxic effects, including apoptosis and growth arrest in spermatogonia, Sertoli cell damage and peritubular cell injury. The results of this study complement the existing basic information on the toxicity of ENU in the testis, and provide scientific information for selecting the appropriate mating time for ENU-treated male mice.

Keywords: ENU (N-ethyl-N-nitrosourea), mouse, testis, histopathological changes, sperm count, ultrastructure

Introduction

The Human Genome Project has revealed that the genetic information required for human life is coded within 30 billion bases. As the next step, an important task of life science researchers is to investigate the functions of all known and unknown genes, especially genes involved in human diseases [1]. The mouse is the major model system used to study the genetics and pathogenesis of human disease, due to the similarity between the mouse and human genomes, biochemical pathways, and pathological mechanisms [2].

ENU (N-ethyl-N-nitrosourea), a laboratory-synthesized compound, is the most effective chemical mutagen in mice, with a mutation rate of 0.0015 per locus per gamete in the commonly used treatment regimes. ENU primarily introduces random, single base pair mutations into the male germ line [3]. Therefore, ENU

mutagenesis is considered to be a relatively promising method for the study of gene function, as mutant mice can be obtained by ENU treatment, and then the mutated genes can be cloned and investigated. Worldwide, several large-scale ENU projects are in the development stages, all of which focus on different biologically-or clinically-relevant phenotypes [4-7].

To establish mutant mouse models using ENU, the first step is to intraperitoneally inject male mice with ENU to induce random mutations, mainly in the spermatogonia. ENU-treated mice usually suffer a period of sterility due to a temporary depletion of spermatogenic cells; however, several weeks after treatment, the surviving spermatogonia repopulate the testis, undergo mitosis and meiosis in the seminiferous tubules and eventually give rise to clones of mutant sperm which can be passed on to future generations. Additionally, at the doses used,

ENU can induce different types of cancer as a bioalkylating agent, which may shorten the life span of the treated mice. The carcinogenicity and duration of sterility induced by ENU are the two major factors which limit its efficiency of mutation. It has been demonstrated that untimely mating results in an increase in mortality of the treated mice; yet, on the other hand, delayed mating may miss the reproductive peak of the treated mice. Therefore, it is obvious that one of the main barriers to ENU mutagenesis is the identification of the ideal mating opportunity, in order to achieve the optimal balance between a high frequency of mutation, the re-establishment of fertility and animal mortality due to cancer [8].

ENU has a variety of effects on different mouse strains, and the inbred strain C57BL/6J has been used successfully in mutagenesis experiments due to its high mutation rate and high toleration for ENU [9]. In order to optimize experimental efficiency, mating should be performed as soon as the treated males regain fertility. In practicality, mating times have largely been decided on the basis of experience, and vary from 5 to 15 weeks after the last injection of ENU [10-12]. The weight, sperm count and morphology of the testis can indicate alterations in fertility, which is helpful for determining suitable mating times. Several studies have reported obvious changes in the testis during the sterile period in ENU-treated mice [13, 14]; however, there is a lack of detailed data, and notably, the ultrastructure of ENU-induced testicular alterations has not been clearly described. Therefore, the aim of the present study was to investigate the effects of ENU on the histopathology of the C57BL/6J male mouse testis using light and transmission electron microscopy, with reference to testis weights and sperm counts. This work is an attempt to complement the preliminary information on ENU toxicity in the mouse testis, and provide a scientific basis for researchers to select the appropriate mating time for ENU-treated mice.

Materials and methods

Ethics statement

This study was conducted in strict accordance with the recommendations given in the Guide for the Care and Use of Laboratory Animals of

the National Research Council. The animal care and use committee of Yangzhou University approved all experiments and procedures conducted on the animals (approval ID: SYXK (Su) 2007-0005).

Animals and treatment

C57BL/6J mice were obtained from the Shanghai Laboratory Animal Center (Shanghai, China). 96 adult male C57BL/6J mice with their weight ranged from 25 to 30 g were used. The animals were randomly divided into two groups: the treatment group (48 mice) and control group (48 mice). The animals in the treatment group were intraperitoneally injected with 100 mg/kg ENU once a week for three consecutive weeks. ENU powder (Sigma) was diluted with phosphate buffer (pH 6.0) to 2 mg/ml, and used immediately after dilution. The animals in the control group were simultaneously injected with PBS alone. Four mice from each group were euthanized each week from week one to week 12 after the first injection, and the testis and cauda epididymis were dissected out for further analysis.

Body and testis weights

The testes and bodies were weighed and the testis/body weight ratio (relative weight of testis) was calculated for each animal.

Sperm counts

To measure the sperm counts, the cauda epididymis were minced and homogenized on ice in 1.0 ml of physiological saline solution with iris scissors until no obvious piece of tissue was visible by eye. The homogenate was filtered, and then 10 μ l of sample was diluted 1:10 in saline solution containing 4% trypan blue and counted under a phase contrast microscope at 200 \times magnification using a haemocytometer [15].

Histopathological and ultrastructural examinations

For light microscopy, the testes of the experimental mice were fixed in 4% paraformaldehyde solution for 24 h, subjected to routine processing for paraffin-embedded tissue samples, sectioned at 3-5 μ m and stained with hematoxylin and eosin [16].

Toxic effects of ENU in the C57BL/6J mouse testes

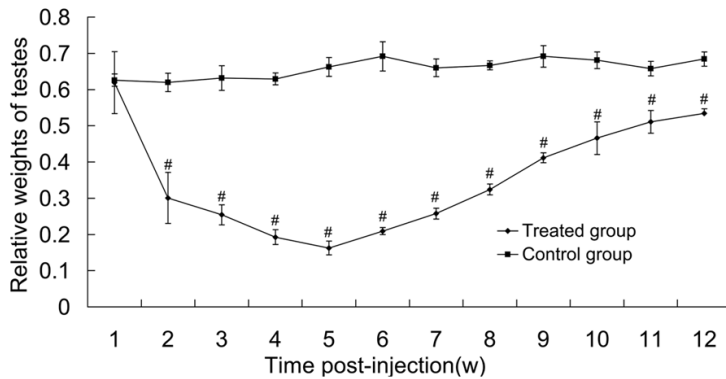


Figure 1. Relative weights of testes of control and ENU-treated mice. * $P < 0.05$ and # $P < 0.01$ vs. control group.

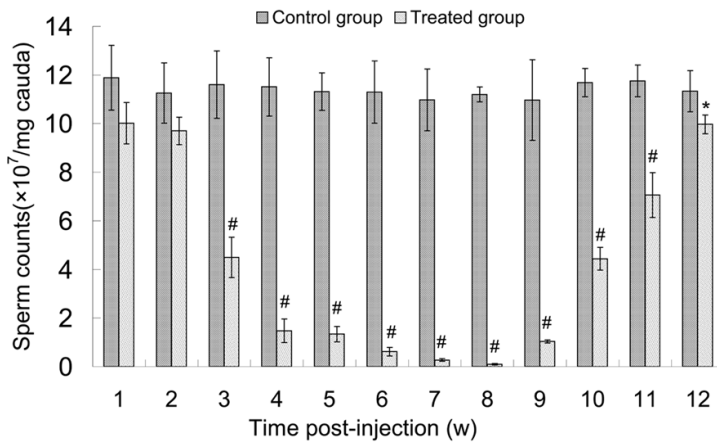


Figure 2. Sperm counts in the cauda epididymis of control and ENU-treated mice. * $P < 0.05$ and # $P < 0.01$ vs. control group.

For electron microscopy, the testes of the experimental mice were fixed in freshly prepared primary fixative containing 2% paraformaldehyde and 2% glutaraldehyde in 0.1 M sodium cacodylate buffer (pH 7.42) containing 0.1% magnesium chloride and 0.05% calcium chloride at 20°C for 10 min, and then transferred to an ice bath for 2 h. The samples were washed three times for 10 min in sodium cacodylate buffer with added chlorides on ice, then subjected to the following steps at room temperature: the testes were subjected secondary fixation for 1 h in 1% osmium tetroxide in sodium cacodylate buffer, washed three times in cacodylate buffer for 30 min, mordanted with 1% tannic acid for 30 min, rinsed with 1% sodium sulphate for 10 min, dehydrated through an ethanol series [20%, 30% (and stained en bloc with 2% uranyl acetate at this stage), 50%, 70%, 90% and 95% ethanol for 20 min each, then 100% ethanol for 20 min three times]. The

ethanol was exchanged with propylene oxide (PO) for 15 min twice, followed by 1:1 PO: Epon resin mixture for at least 1 h, and neat Epon (containing a few drops of PO) overnight. The testes were embedded in fresh resin in a flat moulded tray, cured in an oven at 65°C for 24 h, 40 nm sections were cut using a Leica UCT ultramicrotome, contrasted with uranyl acetate and lead citrate, and imaged on a Tecnai 12 TEM (Philips Co., Netherlands) using a Gatan CCD camera (Gatan Inc., USA) [17].

Statistical analysis

The testis weights and sperm counts are presented as the mean \pm standard deviation (SD) values for each group. Student's t-test was used to analyze the significance between groups. Statistical significance was determined at $P < 0.05$ and $P < 0.01$ level.

Results

Body and testis weights

The body weights of the treatment group and control group were not significantly different throughout the experiment (data not shown); however, significant changes were observed in the testis weights (relative weights of the testes) in the ENU-treated mice (**Figure 1**). In the experimental group, there was a sharp reduction in the testis weights within the first week after the first ENU treatment, and the testis weights continued to gradually decrease until week five post-injection, when the average testis weight in the experimental group was approximately a quarter of the testis weight in the control group. After week five, the testis weights of the experimental group began to increase, and reached nearly 80% of the testis weight of the control group at the end of the experiment (week 12).

Sperm counts

The sperm count of the control mice did not obviously change throughout the experiment;

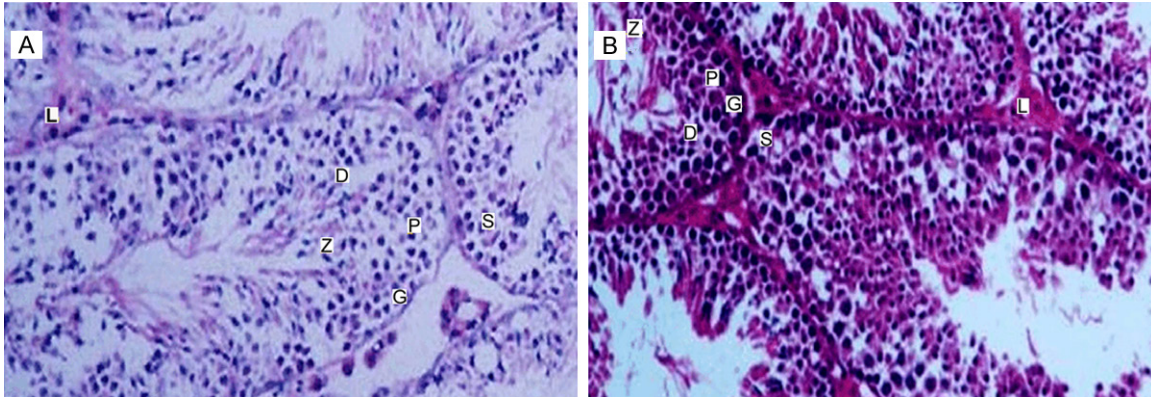


Figure 3. Light micrographs of the testes of control mice. A, B. Note the germinal epithelium formed of regularly arranged rows of spermatogonia, primary spermatocytes and rounded, elongated spermatids, with Sertoli cells observed between the cells. Note the interstitium contains clusters of Leydig cells. G = spermatogonia, S = Sertoli cell, P = primary spermatocyte, L = Leydig cell, D = spermatid, Z = spermatozoa (200 \times , H&E).

however, significant changes were observed in the sperm count of the ENU-treated mice (**Figure 2**). There was no significant difference in the sperm count of the control and experimental groups within the first two weeks after the first injection of ENU; however, the sperm count of the experimental group reduced significantly from week three to week eight post the first injection; the sperm count of the experimental group was close to zero at week eight. The sperm count of the experimental group increased continually from week nine until week 12, and was about 85% of the control group at the end of the experiment (week 12).

Light microscopic examination

Evaluation of hematoxylin and eosin-stained testicular sections from the mice in the control group revealed densely packed seminiferous tubules, with little interstitium, and uniformly sized and shaped tubules. Additionally, the germinal epithelium was formed into regularly arranged rows of spermatogonia, primary spermatocytes, and rounded and elongated spermatids. Sertoli cells could be observed between the cells in the germinal epithelium. The tubules were surrounded by a layer of flat peritubular cells, and the lumina of the tubules contained mature spermatozoa. The interstitium contained clusters of Leydig cells and blood vessels (**Figure 3**).

Light microscopic examination revealed that the histological changes in the testes of the ENU-treated group could be separated into three orderly periods from week one to week

12 after the first injection: the acute period, convalescent period and nearly normal period. The acute period lasted from week one to week four (**Figure 4**). The photomicrographs indicated that the major deleterious effects of ENU on the seminiferous tubules are mainly focused on the spermatogonia. In week one, the normal histoarchitecture of the testis was easily recognized, with the spermatogenic cells layered in an orderly arrangement with the different stages of spermatogenesis observed, and large numbers of mature sperm in the lumina. In week two, though the tubular lumina were filled with mature spermatozoa, the thickness of the seminiferous tubules decreased slightly and fewer cell layers were observed, mainly due to a reduction in the number of spermatogenic cells, compared with the control group. In week three, an obvious reduction in the diameter of the seminiferous tubules was detected, and only Sertoli cells and a small number of spermatogonia were observed near the basement membrane of the germinal epithelium; spermatids and even primary spermatocytes were barely detectable in the shrunken tubules; however, large numbers of mature spermatozoa with their heads pointed toward the base of the lumina and their tails pointed toward the lumina were observed, and spermatocytes detaching from the germinal epithelium were frequently noted. In week four, the histoarchitecture of the testes of the mice in the experimental group was more severely damaged than at any earlier time point, with an apparent decrease in the number of Leydig cells, and only Sertoli cells remaining in the thin walled seminiferous tubules which had a relatively wide lumina and

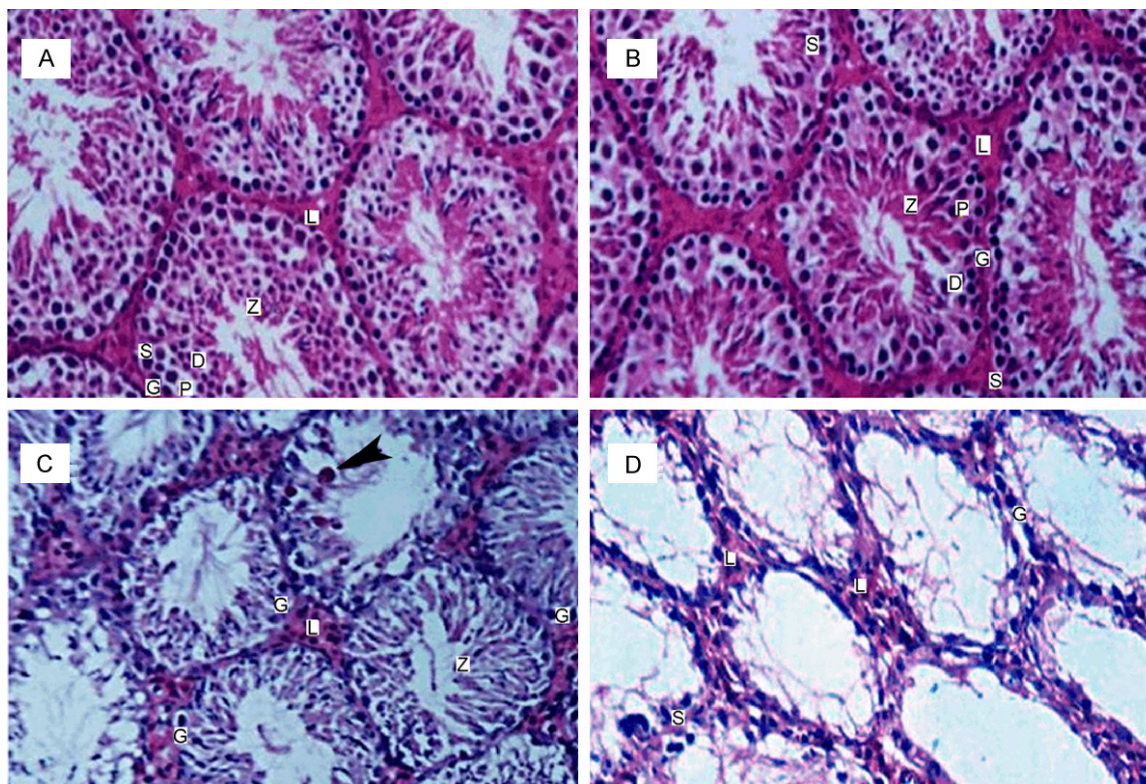


Figure 4. Light micrographs of the testes of ENU-treated mice during the acute period. A. Testicular section at week one after the first injection of ENU. Note the normal histoarchitecture of the testis. B. Testicular section at week two after the first injection of ENU. Note the decreased thickness of the seminiferous tubules and reduced number of cell layers. C. Testicular section at week three after the first injection of ENU. Note large numbers of spermatozoa with their heads pointed toward the base of the lumina and tails pointed toward the lumina, and spermatocytes (thick arrow) detaching from the germinal epithelium. D. Testicular section at week four after the first injection of ENU. Note Sertoli cells are only present in thin walled seminiferous tubules with relatively wide lumina, which lack mature spermatozoa and contains vacuoles of variable sizes. G = spermatogonia, S = Sertoli cell, P = primary spermatocyte, L = Leydig cell, D = spermatid, Z = spermatozoa (200 \times , H&E).

did not contain any mature spermatozoa but only vacuoles of variable sizes.

The acute period was followed by the convalescent period, which lasted from week five to week eight (**Figure 5**). In week five, further atrophy of the seminiferous tubules was observed; however, two features indicated that the testes of the ENU-treated group were entering a recovery phase. Firstly, the interstitial space became wider and filled with Leydig cells; secondly, clusters of spermatogonia which were propagated from division of the surviving spermatogonia were observed near the basement membrane of the seminiferous tubules. In week six, the interstitial space was still filled with Leydig cells, and the diameter of the seminiferous tubules was still smaller than that of the control group. Several layers of spermatogenic cells

were located in the brim of the seminiferous tubules and dividing nuclei were frequently detected. Quite a few intercellular vacuolations were observed in the germinal epithelium, however, spermatids and mature spermatozoa had not yet appeared in the lumina. In week seven, the number of Leydig cells in the interstitial space was still higher than the control group, though the diameter of the seminiferous tubules had returned to almost normal, and spermatogonia, primary spermatocytes, spermatids and small numbers of mature spermatozoa could be observed in an orderly arrangement in the tubules. In week eight, the epithelial height, an indicator of normal spermatogenesis, had increased further compared with week seven, and the number of Leydig cells had almost returned to similar numbers as control mice.

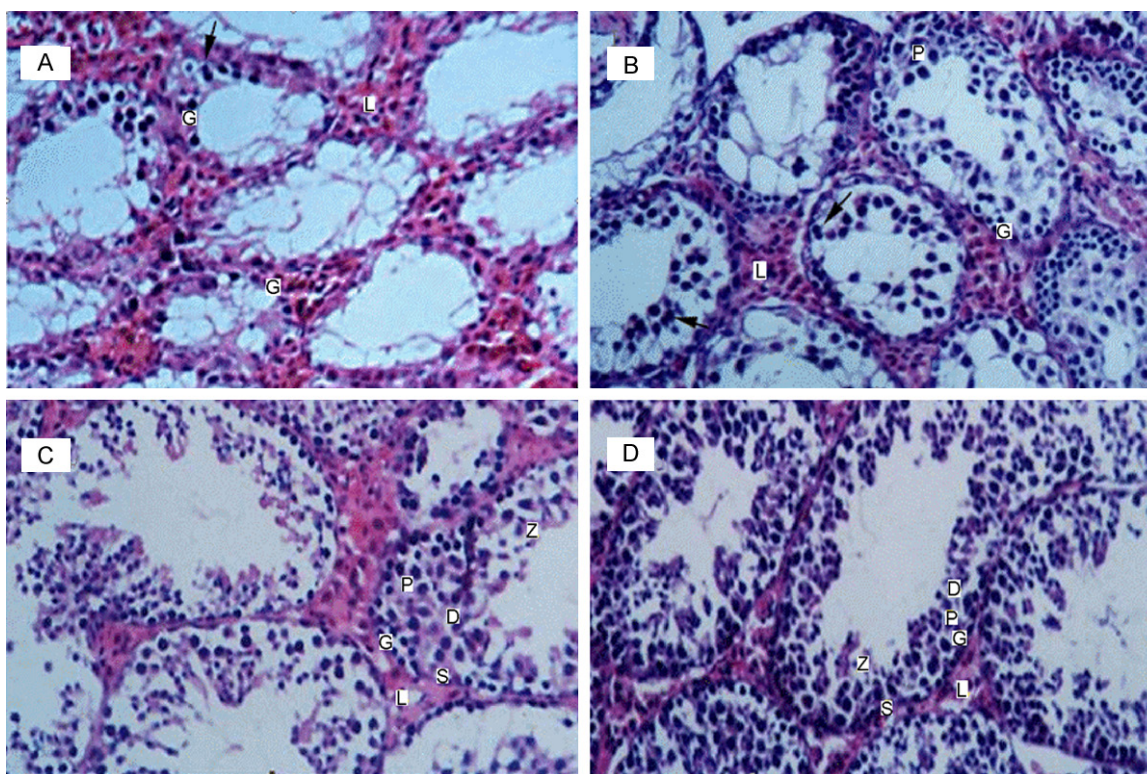


Figure 5. Light micrographs of the testes of ENU-treated mice during the convalescent period. A. Testicular section at week five after the first injection of ENU. Note the widened interstitial space filled with Leydig cells, and the clusters of spermatogonia propagated from division of the surviving spermatogonia. Also note the frequent dividing nuclei (thin arrow). B. Testicular section at week six after the first injection of ENU. Note the interstitial space overgrown with Leydig cells and several layers of spermatogenic cells located in the brim of the seminiferous tubules. Note frequent dividing nuclei (thin arrow) and the lumina lacking spermatids or mature spermatozoa. C. Testicular section at week seven after the first injection of ENU. Note the spermatogonia, primary spermatocytes, spermatids and even a small number of mature spermatozoa arranged in an orderly manner in the tubules. D. Testicular section at week eight after the first injection of ENU. Note the increased epithelial height and almost all types of spermatogenic cells arranged in an orderly manner within the tubules. G = spermatogonia, S = Sertoli cell, P = primary spermatocyte, L = Leydig cell, D = spermatid, Z = spermatozoa (200 \times , H&E).

The third stage, the nearly normal period, lasted from week nine to week 12. During this period, the photomicrographs revealed that the testes of the ENU-treated group had nearly regained a normal architecture. The seminiferous tubules were packed together and defined by regular outlines, and the narrow interstitium contained normal Leydig cells. Most of the seminiferous tubules had restored to the normal epithelial stratification with layers of spermatogenic cells at different developmental stages, and the major structural feature of this period was the appearance of a moderate number of mature spermatozoa in the lumina (figures not shown).

Electron microscopy

Electron microscopic examination revealed the normal ultrastructure of the testes of the mice

in the control group (**Figure 6**). The seminiferous tubules were bounded by elongated peritubular cells and encircled by a regular, continuous basement membrane. Sertoli cells were identified by their large indented nuclei, and their cytoplasm contained numerous mitochondria, smooth endoplasmic reticulum, a few lysosomes and lipid droplets. Specialized junctional complexes between adjacent Sertoli cells were observed, and the basal compartment and adluminal compartment were easily distinguished. Spermatogonia with rounded nuclei and some mitochondria were detected close to the basement membrane. Primary spermatocytes appeared above the spermatogonia as larger rounded cells with a thin rim of cytoplasm and large rounded nuclei containing synaptonemal complexes. Spermatids at different stages of differentiation were noted. Early spermatids appeared rounded in shape and smaller than

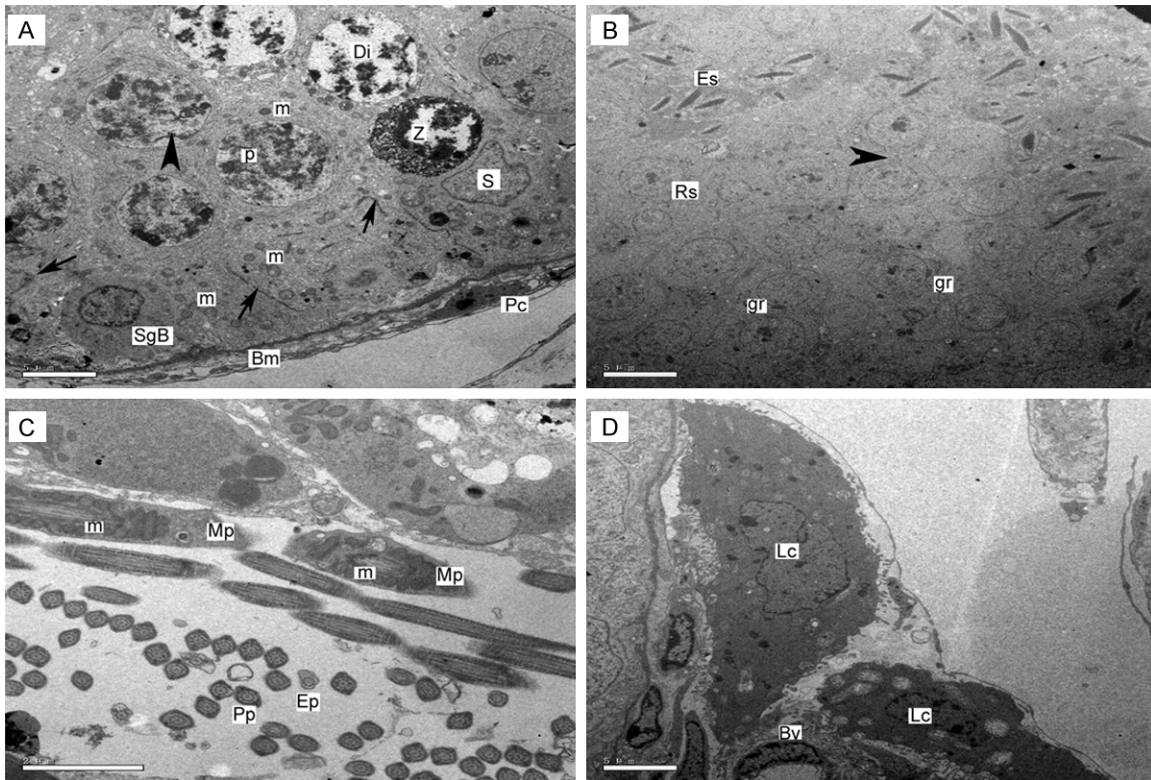


Figure 6. Electron micrographs of the testes of control mice. A. Part of a seminiferous tubule with type B spermatogonia in the basal compartment between adjacent Sertoli cells attached by tight junctions (thin arrows). The Sertoli cells rest on the basement membrane. Note zygotene spermatocytes, diplotene spermatocytes, pachytene spermatocytes with a synaptonemal complex (thick arrow) and mitochondria. B. Part of a seminiferous tubule with an intercellular bridge (thick arrow) observed between two round spermatids. Early differentiating spermatid with an acrosomal granule and an acrosomal vesicle spreading over a rounded nucleus, and elongating spermatids with strongly elongated condensed nuclei covered anteriorly by the acrosome cap. C. Sections of the tail of spermatids. Note the longitudinal sections of the middle pieces of the tail of the spermatids with mitochondrial sheaths, and the cross sections of the principal and end pieces. D. Part of the interstitium between seminiferous tubules. Note Leydig cells with cytoplasm containing a few lipid droplets and mitochondria around the blood vessels. SgB = spermatogonia type B, S = Sertoli cell, Bm = basement membrane, Z = zygotene spermatocyte, Di = diplotene spermatocyte, P = pachytene spermatocyte, m = mitochondria, Rs = round spermatid, gr = acrosomal granule, Es = elongating spermatid, Mp = middle piece of the spermatids' tail, Pp = principal piece of the spermatids' tail, Ep = end piece of the spermatids' tail, Lc = Leydig cell, Ld = lipid droplet, Bv = blood vessels.

primary spermatocytes. The nuclei of early spermatids were suffused with evenly distributed chromatin. Intercellular bridges could be observed connecting adjacent spermatids. The cytoplasm of spermatids contained numerous well developed Golgi apparatus and mitochondria. Differentiating spermatids contained developing acrosomes that appeared as acrosomal granules and acrosomal vesicles adhered to the pole of the rounded nuclei. Acrosomal caps, resulting from spreading of the acrosomal vesicle, appeared covering one hemisphere of the nuclei of differentiating spermatids. Elongation of the nuclei of the spermatids during the process of spermiogenesis was

observed. The heads of late elongating spermatids contained strongly elongated, electron-dense nuclei covered anteriorly by acrosome caps. Longitudinal or cross-sections through the tails of developing spermatozoa revealed that the tails were surrounded by the remnants of the cytoplasm of spermatids or Sertoli cells. Transverse sections of different spermatozoa showed that the mid, principal and end pieces had a central axoneme formed from nine doublets of microtubules with two central singlets. In the mid-piece of the spermatozoa, the axoneme was surrounded by nine dense bundles of fibrous and mitochondrial sheaths. In the principal piece of the spermatozoa, the axo-

Toxic effects of ENU in the C57BL/6J mouse testes

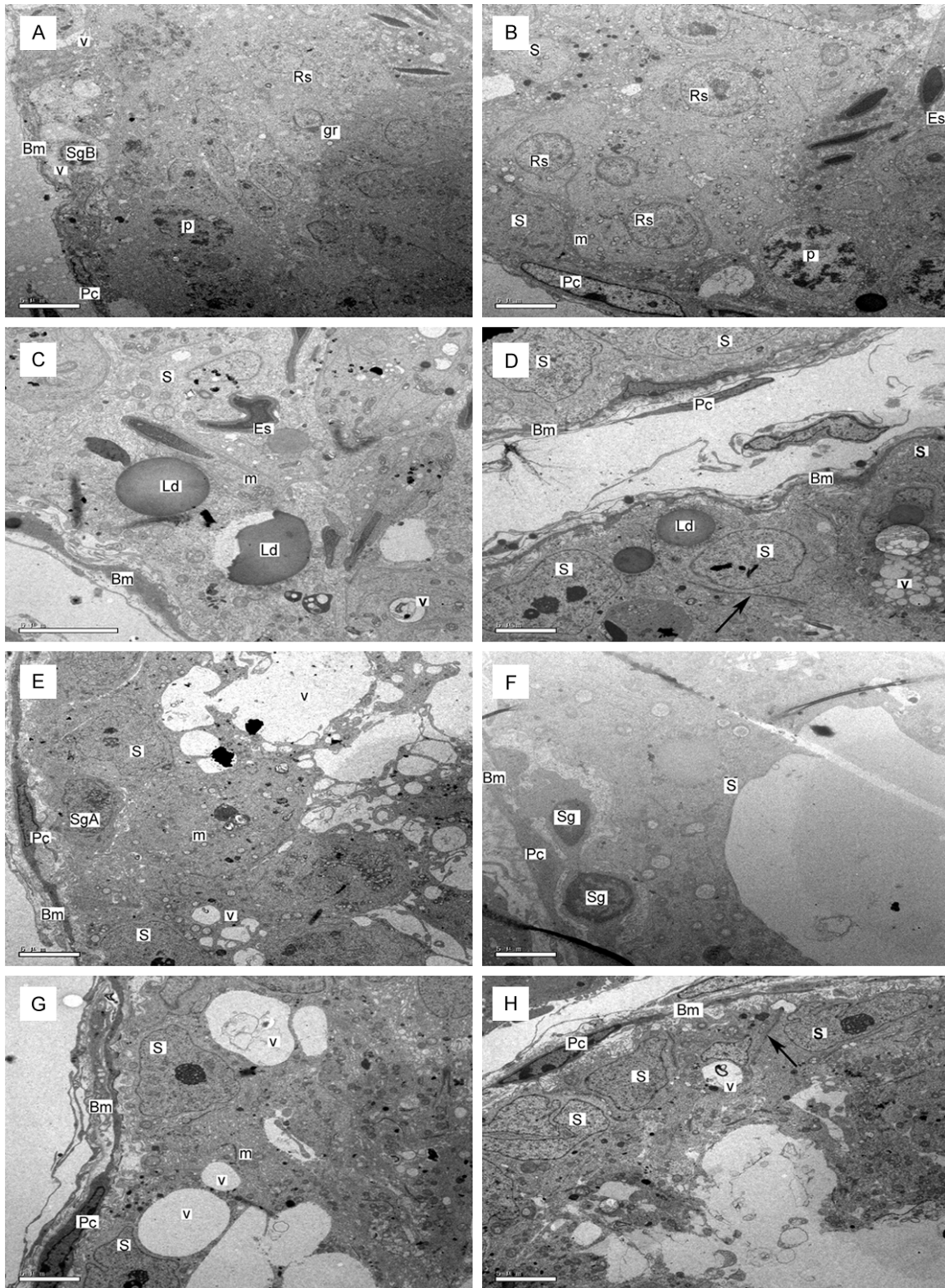


Figure 7. Electron micrographs of the testes of ENU-treated mice during the acute period. A. Part of a seminiferous tubule at week one after the first injection of ENU. Note the infolded basement membrane and large vacuoles in the disintegrated cytoplasm of type B spermatogonia. B. Part of a seminiferous tubule at week two after the first injection of ENU. Note the primary spermatocytes and round spermatids aberrantly close to the basement membrane. C. Part of a seminiferous tubule at week three after the first injection of ENU. Note the elongating spermatids with dis-

Toxic effects of ENU in the C57BL/6J mouse testes

rupted and irregular nuclear membrane and involuted acrosome located near the ruptured basement membrane, and large lipid droplets and vacuoles in the cytoplasm of Sertoli cells. D-H. Parts of seminiferous tubules at week four after the first injection of ENU. Note Sertoli cells resting on the basement membrane with their cytoplasmic extensions nearly forming a continuous single cell layer (G, H). Lipid droplets, large vacuoles containing membranous material, and swollen mitochondria with widened cristae are observed within the cytoplasm of Sertoli cells (D, G and H). Note specialized junctional complexes (thin arrows) between adjacent Sertoli cells (D, H), and atrophic spermatogonia with reduced numbers of organelles, vacuolated cytoplasm and shrunken pyknotic nuclei (F). Apparently normal spermatogonia with oval nuclei and diffused chromatin can be observed between Sertoli cells (E). SgA = type A spermatogonia, SgB = type B spermatogonia, Sg = spermatogonia, S = Sertoli cell, Bm = basement membrane, P = primary spermatocyte, m = mitochondria, Rs = round spermatid, gr = acrosomal granule, Es = elongating spermatid, Ld= lipid droplet, v = vacuole.

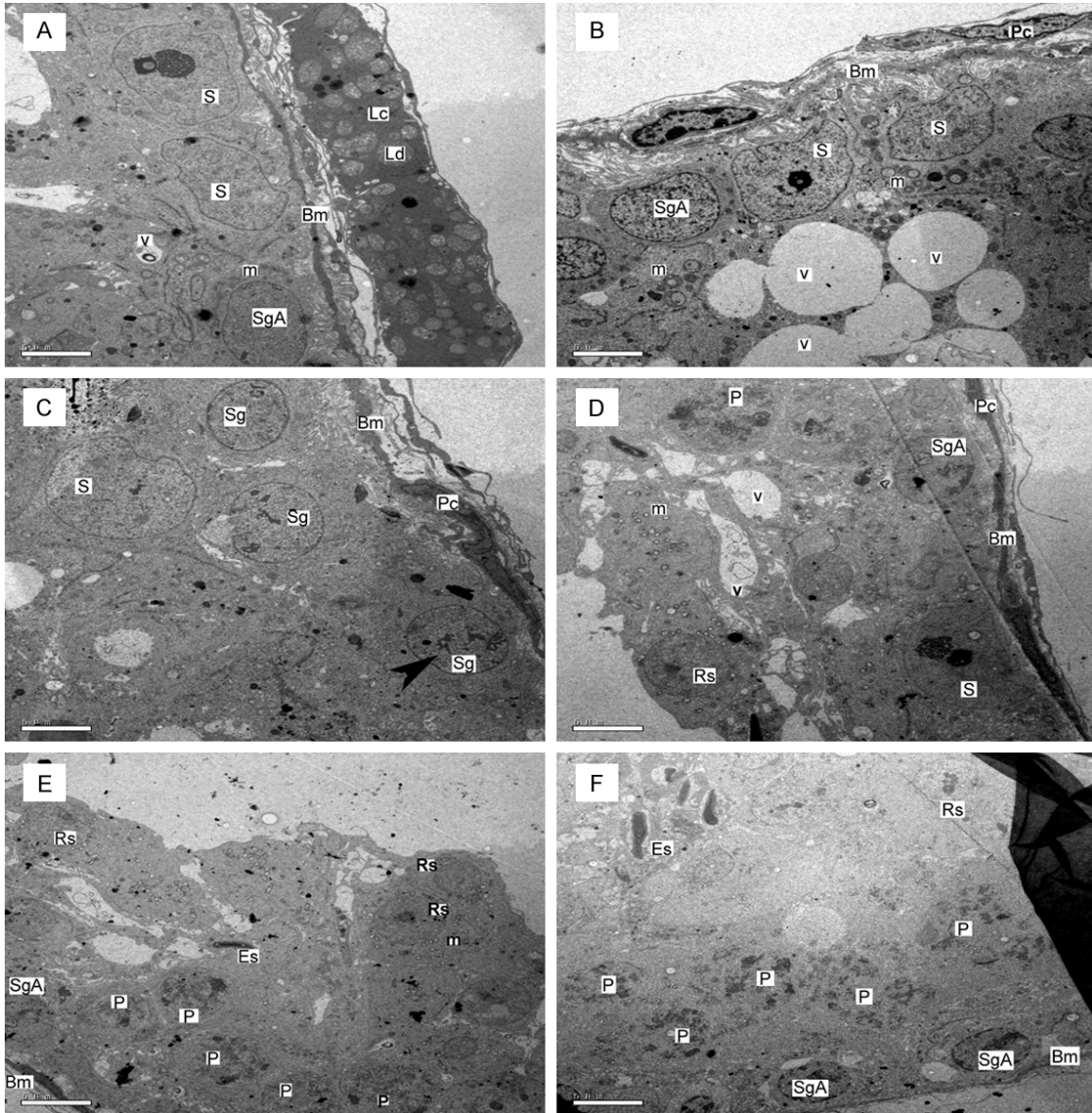


Figure 8. Electron micrographs of the testes of ENU-treated mice during the convalescent period. A, B. Parts of seminiferous tubules at week five after the first injection of ENU. Note spermatogonia with round euchromatic nuclei and tubular mitochondria appearing in the basal compartment of the seminiferous tubules. C. Part of a seminiferous tubule at week six after the first injection of ENU. Note dividing spermatogonia with chromosomes (thick arrow) arranged on the equatorial plate. D, E. Parts of seminiferous tubules at week seven after the first injection of ENU. Note all types of spermatogenic cells, including spermatogonia, spermatocytes, spermatids and even a few elongating spermatids with a normal ultrastructure in the seminiferous tubules; however, the tubules are only formed by

Toxic effects of ENU in the C57BL/6J mouse testes

three or four layers of spermatogenic cells. F. Part of a seminiferous tubule at week eight after the first injection of ENU. Note the nearly normal ultrastructure of the germinal epithelium. SgA = type A spermatogonia, SgB = type B spermatogonia, Sg = spermatogonia, S = Sertoli cell, Bm = basement membrane, P = primary spermatocyte, m = mitochondria, Rs = round spermatid, Es = elongating spermatid, Ld = lipid droplet, v = vacuole.

neme was only surrounded by the fibrous sheath. Leydig cells contained irregular nuclei with a thin rim of peripheral heterochromatin, and their cytoplasm contained a few lipid droplets and mitochondria with tubular cristae.

The histopathological effects of ENU on the testis were confirmed at the ultrastructural level. Electron photomicrographs of testicular sections from the experimental group revealed severe and extensive histological abnormalities which increased over time during the acute period (**Figure 7**). In week one after the first injection of ENU, there were no significant abnormalities in the ultrastructure of the seminiferous tubules, except for an irregular, infolded basement membrane and enlarged vacuoles within the disintegrated cytoplasm of the spermatogonia. In week two, aberrant primary spermatocytes were detected close to the basement membrane, and rounded and elongated spermatids were observed at an inappropriate depth within the epithelium; however, these cells possessed an approximately normal ultrastructure. In week three, in addition to the inappropriate location of spermatids, which were even located near to the ruptured basement membranes, there was an obvious reduction in the number of spermatocytes. Furthermore, undifferentiated spermatogonia were rarely detected and intercellular spaces and intracellular vacuoles were observed in the tubules, while large lipid droplets appeared in the cytoplasm of Sertoli cells. Elongating spermatids with disrupted, irregular nuclear membranes and involuted acrosomes were surrounded by Sertoli cell cytoplasm. In week four, the most notable morphological alteration was that the seminiferous tubules were comprised almost entirely of Sertoli cells resting on the basement membrane, with the cytoplasmic extensions of the Sertoli cells nearly forming a continuous single layer of cells. Electron-dense material, lipid droplets of variable sizes, large vacuoles containing membranous material, and swollen mitochondria with widened cristae were observed within the cytoplasm of Sertoli cells; meanwhile, the specialized junctional complexes between adjacent Sertoli cells appeared to be intact. Atrophic spermatogonia

with an overall reduced number of organelles, vacuolated cytoplasm and shrunken pyknotic nuclei were recognized by their location, and occasionally, apparently normal spermatogonia with diffused chromatin were apparent between Sertoli cells. Moreover, other abnormalities were observed at week four, including: (1) irregular basement membrane of seminiferous tubules with relatively thick or thin patches, (2) shrunken testicular peritubular cells which had lost their characteristic long, narrow "spindle" shape, with nuclei containing dark patches, some of which detached from the interstitial tissue, (3) a complete loss of spermatocytes, spermatids and mature spermatozoa, and (4) abnormal cellular debris in the tubular lumina.

In week five, the first week of the convalescent period, the obvious histological characteristic compared to week four was the multiplication of spermatogonia. Compared to the abnormal ultrastructure of the acute period, two or three spermatogonia with round euchromatic nuclei and tubular mitochondria appeared in the basal compartment of the seminiferous tubules. In week six, additional spermatogonia were observed, accompanied by dividing spermatogonia with chromosomes arranged on the equatorial plate, strongly suggestive of cell proliferation. Moreover, Leydig cells with large numbers of lipid droplets and variable-size electron-dense granules appeared to interdigitate with the neighboring Leydig cells. In week seven, all types of spermatogenic cells including spermatogonia, spermatocytes, round spermatids and even a few elongating spermatids with a normal ultrastructure were observed to be correctly arranged within the epithelium of the seminiferous tubules; however, the tubules were only formed by three or four layers of spermatogenic cells, so the number of cells was significantly lower than that in the testes of control mice. Intercellular separations and intracellular vacuoles could still be observed in Sertoli and spermatogenic cells, while the basement membrane became smooth and regular. In week eight, the number of spermatogenic cells increased further, and compared to the ultrastructure at week seven, organelles such as the mitochondria and endoplasmic reticulum became more abundant and typical (**Figure 8**).

Electron photomicrographs of sections prepared from experimental mice during week nine to week 12 revealed the overall normal-like ultrastructure of the testes during the nearly normal period (figures not shown).

Discussion

Given the high degree of similarity between the mouse and human genomes, biochemical pathways and pathological mechanisms, the mouse is the major model system used for obtaining insight into the functions of human genes, primarily through the use of mutant mouse models [2]. Currently, the majority of mutant mice strains are knockout animals; however, these valuable models are only likely to represent a small proportion of the total number of human genes. This gap is being partially filled by the establishment of new mutagenesis programs using potent mutagens such as ENU. ENU, an alkylating agent, has been found to be a powerful mutagen in mouse spermatogonia [3]. In this study, we demonstrated that ENU exerts time-dependent effects on mouse testis weights and sperm counts, which correlated with the severity of the histopathological and ultrastructural changes in the testes.

A reduction in the testis weight may be attributed to decreased sperm production [18], and an appropriate sperm count is one of the key factors for mating success. In our research, the testis weights and sperm counts of the ENU-treated mice drastically reduced at first several weeks and then had restored to around 80% of the respective values in the control group by the end of the experiment. In the mouse, differentiating spermatogonia undergo a precisely timed sequence of mitotic divisions and differentiation towards the formation of spermatozoa, and then the spermatozoa are released from the seminiferous tubules into the epididymis for further maturation. The evolution of stem-cell spermatogonia into mature sperm takes approximately 43 days (about six weeks). In the present study, light microscopic examination revealed that a small number of sperm reappeared in the seminiferous tubules around five to six weeks after the last the injection of ENU (weeks seven/eight after the first injection), which was about six weeks for the surviving spermatogonia to differentiate into mature sperm.

Notably, within our 12-week experiment, none of the ENU-treated animals recovered the normal testis weights or sperm counts observed in the control animals. Thus, we conclude that the testis has the ability to regain a generally normal architecture after the removal of ENU, but that the recovery of spermatogenesis was incomplete within 12 weeks of the first injection. We deduce that large numbers of spermatogonial stem cells are killed during the toxin insult, otherwise spermatogenesis would recover more rapidly and completely.

Histological examination demonstrated variable adverse effects in the testes of the ENU-treated mice. Under light microscopic examination, the seminiferous tubules were observed to undergo time-dependent morphological changes, with distinct injury and recovery phases. The abnormalities observed during the acute period were in agreement with the literature reports that ENU predominantly affects premeiotic spermatogonia which have higher mitotic rate, not spermatogenic cells undergoing or that have undergone meiosis [19]. In this study, there were large numbers of sperm with a complete absence of spermatids and spermatocytes in the shrunken tubules at week three, and in week four, there were only Sertoli cells without any spermatogenic cells. These observations might be explained by the fact that ENU-induced damage to premeiotic spermatogonia hinders subsequent spermatogenesis, while spermatogenic cells undergoing or which had undergone meiosis were depleted, which contributed to the temporary sterile period. The most severe damage was detected four weeks after the first injection of ENU, in the form of thinning of the epithelial wall, widening of the lumen contained large vacuoles, and shrinking of the peritubular cells; the most notable abnormality was the presence of only Sertoli cells in the seminiferous tubules. The histological changes during the convalescent period were characterized by reconstruction of the seminiferous tubules, and overgrowth of Leydig cells which regulate spermatogenesis by synthesizing and secreting testosterone [20].

Moreover, electron microscopy confirmed the time-dependent toxic effects of ENU at an ultrastructural level. The ultrastructural abnormalities observed during the acute period were severe and extensive; the most serious altera-

tions appeared at week four, mainly including: (1) Sertoli cells nearly forming a continuous single cell layer, with electron-dense material, swollen mitochondria and large vacuoles in the cytoplasm, (2) atrophic spermatogonia with reduced numbers of organelles, a vacuolated cytoplasm and shrunken pyknotic nuclei located near the irregular basement membrane, (3) shrunken testicular peritubular cells detaching from the interstitial tissue, and (4) a total absence of primary spermatocytes, spermatids and sperm. However, the specialized junctional complexes between adjacent Sertoli cells appeared to remain intact at all times during the entire experiment, which indicates that Sertoli cells were not totally destroyed by ENU and had the ability to recover normal function relatively quickly. At week four, a small number of apparently normal spermatogonia containing diffused chromatin were noticed between Sertoli cells; these spermatogonia might be mutant spermatogonia which survived ENU treatment and retained the ability to differentiate into mutant sperm that can be passed on to future generations.

Apoptosis is a physiological process of cell death that contributes to the maintenance of cell number and helps to remove damaged cells; however, excessive apoptosis in the testis can reduce male reproductive function [21]. We observed apoptotic spermatogonia with characteristic shrunken pyknotic nuclei, concentrated cell plasma and aggregated organelles, in accordance with Katayam' et al [22], who reported that the monofunctional alkylating agent ENU induced apoptosis and growth arrest in rat tissues. ENU is highly mutagenic, and induces apoptosis after S-phase accumulation in a p53-dependent manner in response to DNA-damage [23]. In this research, apoptosis was apparent in the spermatogonia, but was not detected in other cell types such as Sertoli cells or spermatocytes. This result could be explained by the previous literature, in which differentiating spermatogonia were regarded to be most sensitive testicular cells to ENU damage, because of their higher mitotic rate compared to other spermatogenic cells and non-proliferating Sertoli cells [19]. The apoptosis of the spermatogonia might be a possible reason for the incomplete recovery of spermatogenesis observed in ENU-treated mice in this study.

In the present study, depletion of germ cells and cytoplasmic vacuolations in Sertoli cells were extremely striking abnormalities in week four. Depletion of germ cells could be attributed to the apoptosis and growth arrest of spermatogonia, and cytoplasmic vacuolations in Sertoli cells were previously hypothesized to be derived from dilatation and vesiculation of the smooth endoplasmic reticulum [24]. This dilatation might be due to the ingress of water into the cell as a part of hydropic degeneration, a change that might occur in Sertoli cells in response to ENU. In addition, Creasy [25] revealed that vacuolations of Sertoli cells were an early and common morphological response to injury. Sertoli cells play a very important role in spermatogenesis by regulating the immediate environment of the developing germ cells, by providing physical support, junctional complexes or barriers, and/or biochemical stimulation in the form of growth actors or nutrients. Thus, the Sertoli cell damage observed in the present study may lead to an insufficient supply of nutrients to spermatogenic cells, which may explain the separation of spermatocytes from Sertoli cells and structural alterations observed in spermatogenic cells. Additionally, any injury affecting Sertoli cells [26] will also exert a rapid secondary effect on the production of a host of proteins that regulate and/or respond to pituitary hormone release, which could subsequently inhibit spermatogenesis, and lead to abnormalities and the death of spermatogenic cells.

Additionally, the cytoplasmic vacuolations in Sertoli cells and spermatogenic cell abnormalities observed in response to ENU in the current study may be a result of peritubular cell injury. Electron microscopy demonstrated that the shrunken peritubular cells with abnormal dark, patched nuclei totally lost their characteristic long, narrow "spindle" shape. Testicular peritubular cells are myofibroblast-like cells that surround the seminiferous tubules and are responsible for tubular contractility and sperm transport. Recently, several reports have augmented this simplified view, by showing that peritubular cells are not only structural cells but also actively produce paracrine mediators. Studies have suggested that these paracrine mediators influence the homeostasis of the testicular environment, and modulate testicular morphology and Sertoli cell function [27]. Thus, the changes observed in peritubular cells in the

present study adds further information to the mechanisms by which ENU induces damage to the architecture of the seminiferous tubules.

In summary, treatment with 100 mg/kg ENU weekly for three weeks altered spermatogenesis, which in turn affected the fertility of male C57BL/6J mice. The time-dependent changes in the testis weights, sperm counts and testicular morphology followed a pattern of injury and recovery. The most severe damage was a temporary depletion of spermatogenic cells, which was identified by both light and electron microscopy, and can be directly or indirectly attributed to the toxic effects of ENU. Based on the sperm counts and analysis of testicular morphology, we conclude that the optimal mating time should be scheduled at least six after weeks after the last injection of ENU. Our conclusive results complement the existing basic information on the mechanisms of ENU toxicity in the mouse testis, and provide scientific information for researchers to select the appropriate mating times for ENU-treated mice.

Acknowledgements

This work was supported by a grant from the National Natural Science Foundation of China (31201864), and by a project funded by the Priority Academic Program Development of Jiangsu Higher Education Institutions.

Disclosure of conflict of interest

None.

Address correspondence to: Dr. Jun Yin, College of Veterinary Medicine, Yangzhou University, 12# Wenhui, East Road, Yangzhou 225009, Jiangsu, PR China. Tel: +86-0514-87979384; Fax: +86-0514-87972218; E-mail: sy-yinjun@163.com

References

- [1] Lander ES. Initial impact of the sequencing of the human genome. *Nature* 2011; 470: 187-197.
- [2] Emes RD, Goodstadt L, Winter EE, Ponting CP. Comparison of the genomes of human and mouse lays the foundation of genome zoology. *Hum Mol Genet* 2003; 12: 701-709.
- [3] Rinchik EM. Chemical mutagenesis and fine-structure functional analysis of the mouse genome. *Trends Genet* 1991; 7: 15-21.
- [4] Reinholdt L, Ashley T, Schimenti J, Shima N. Forward genetic screens for meiotic and mitotic recombination-defective mutants in mice. *Methods Mol Biol* 2004; 262: 87-107.
- [5] Kile BT, Hentges KE, Clark AT, Nakamura H, Saling AP, Liu B, Box N, Stockton DW, Johnson RL, Behringer RR, Bradley A, Justice MJ. Functional genetic analysis of mouse chromosome 11. *Nature* 2003; 425: 81-86.
- [6] Inoue M, Sakuraba Y, Motegi H, Kubota N, Toki H, Matsui J, Toyoda Y, Miwa I, Terauchi Y, Kadowaki T, Shigeyama Y, Kasuga M, Adachi T, Fujimoto N, Matsumoto R, Tsuchihashi K, Kagami T, Inoue A, Kaneda H, Ishijima J, Masuya H, Suzuki T, Wakana S, Gondo Y, Minowa O, Shi-roishi T, Noda T. A series of maturity onset diabetes of the young, type 2 (MODY2) mouse models generated by a large-scale ENU mutagenesis program. *Hum Mol Genet* 2004; 13: 1147-1157.
- [7] Cook MC, Vinuesa CG, Goodnow CC. ENU-mutagenesis: insight into immune function and pathology. *Curr Opin Immunol* 2006; 18: 627-633.
- [8] Balling R. ENU mutagenesis: analyzing gene function in mice. *Annu Rev Genomics Hum Genet* 2001; 2: 463-492.
- [9] Justice MJ, Carpenter DA, Favor J, Neuhauser-Klaus A, Hrabe de Angelis M, Soewarto D, Moser A, Cordes S, Miller D, Chapman V, Weber JS, Rinchik EM, Hunsicker PR, Russell WL, Bode VC. Effects of ENU dosage on mouse strains. *Mamm Genome* 2000; 11: 484-488.
- [10] Wansleeben C, van Gulp L, de Graaf P, Mouson F, Marc Timmers HT, Meijlink F. An ENU-induced point mutation in the mouse *Btaf1* gene causes post-gastrulation embryonic lethality and protein instability. *Mech Dev* 2011; 128: 279-288.
- [11] Rathkolb B, Fuchs E, Kolb HJ, Renner-Muller I, Krebs O, Balling R, Hrabe de Angelis M, Wolf E. Large-scale N-ethyl-N-nitrosourea mutagenesis of mice—from phenotypes to genes. *Exp Physiol* 2000; 85: 635-644.
- [12] Brown FC, Scott N, Rank G, Collinge JE, Vado-las J, Vickaryous N, Whitelaw N, Whitelaw E, Kile BT, Jane SM, Curtis DJ. ENU mutagenesis identifies the first mouse mutants reproducing human beta-thalassemia at the genomic level. *Blood Cells Mol Dis* 2013; 50: 86-92.
- [13] Rodriguez M, Panda BB, Ficsor G. Testes weight reflect ethylnitrosourea induced histopathology in mice. *Toxicol Lett* 1983; 17: 77-80.
- [14] Oakberg EF, Crosthwait CD. The effect of ethyl-, methyl- and hydroxyethyl-nitrosourea on the mouse testis. *Mutat Res* 1983; 108: 337-344.
- [15] Swayne BG, Kawata A, Behan NA, Williams A, Wade MG, Macfarlane AJ, Yauk CL. Investigat-

Toxic effects of ENU in the C57BL/6J mouse testes

- ing the effects of dietary folic acid on sperm count, DNA damage and mutation in Balb/c mice. *Mutat Res* 2012; 737: 1-7.
- [16] Carleton HM. *Histological technique*. London: Oxford University Press; 1957.
- [17] Bozzola JJ, Russell LD. *Electron microscopy: principles and techniques for biologists*. Jones & Bartlett Learning 1999.
- [18] Yeh YC, Lai HC, Ting CT, Lee WL, Wang LC, Wang KY, Lai HC, Liu TJ. Protection by doxycycline against doxorubicin-induced oxidative stress and apoptosis in mouse testes. *Biochem Pharmacol* 2007; 74: 969-980.
- [19] Russell WL, Kelly EM, Hunsicker PR, Bangham JW, Maddux SC, Phipps EL. Specific-locus test shows ethylnitrosourea to be the most potent mutagen in the mouse. *National Acad Scienc* 1979: 5818-5819.
- [20] Goji K, Tanikaze S. Spontaneous gonadotropin and testosterone concentration profiles in prepubertal and pubertal boys: temporal relationship between luteinizing hormone and testosterone. *Pediatr Res* 1993; 34: 229-236.
- [21] Aitken RJ, Findlay JK, Hutt KJ, Kerr JB. Apoptosis in the germ line. *Reproduction* 2011; 141: 139-150.
- [22] Katayama K, Ishigami N, Suzuki M, Ohtsuka R, Kiatipattanasakul W, Nakayama H, Doi K. Teratologic studies on rat perinates and offspring from dams treated with ethylnitrosourea (ENU). *Exp Anim* 2000; 49: 181-187.
- [23] Katayama K, Ueno M, Yamauchi H, Nakayama H, Doi K. Ethylnitrosourea-induced apoptosis in primordial germ cells of the rat fetus. *Exp Toxicol Pathol* 2002; 54: 193-196.
- [24] Murthy RC, Saxena DK, Gupta SK, Chandra SV. Lead induced ultrastructural changes in the testis of rats. *Exp Pathol* 1991; 42: 95-100.
- [25] Creasy DM. Pathogenesis of male reproductive toxicity. *Toxicol Pathol* 2001; 29: 64-76.
- [26] Johnson L, Thompson DL Jr, Varner DD. Role of Sertoli cell number and function on regulation of spermatogenesis. *Anim Reprod Sci* 2008; 105: 23-51.
- [27] Reid LM, Jefferson DM. Cell culture studies using extracts of extracellular matrix to study growth and differentiation in mammalian cells. *Mammalian cell culture*. Springer; 1984. pp. 239-280.